MULTI-SPACECRAFT VALIDATION OF A CURRENT SHEET MODEL

J. De Keyser, M. Roth

Belgian Institute for Space Aeronomy, Ringlaan 3, B-1180 Brussels, Belgium

ABSTRACT

We have developed a kinetic equilibrium model that describes current sheet structure in the widely different plasma regimes found in the solar wind and in geospace. In this paper we review the techniques that we have used to validate our model. The generality of the model forced us to consider current sheets in various regimes. The validation process included observations of solar wind current sheets (ULYSSES and WIND) and of the magnetopause (ISEE-1 and -2 and AMPTE/IRM). The availability of a validated model describing current sheets under various circumstances allows us to make general conclusions regarding the existence and the structure of current sheet equilibria.

Key words: current sheets; plasma discontinuities.

1. INTRODUCTION

Thin boundary layers separate regions in space filled with distinct plasmas. A boundary layer is characterized by multiple thickness scales, of the order of the gyroradii of the particles on either side of the interface. The currents flowing inside the layer are related to magnetic field changes across the boundary. The structure of a current sheet is strongly affected by the composition and temperatures of the plasmas involved. Magnetic field and plasma bulk flow conditions on either side of the interface also play an important role. The properties of current sheets in different regions in the heliosphere and in geospace may therefore be very different.

Satellite instruments that intend to investigate the physical processes operating in boundary layers must be designed for and operated at sufficiently high data rates in order to be able to resolve the internal structure of current sheets. The requirements are different for an instrument observing solar wind current sheets close to or far from the Sun, or looking at the magnetopause. At the same time there may be specific operational constraints. For instance, because of satellite power budget constraints, telemetry requirements for satellites in heliospheric orbit (e.g., ULYSSES) result in relatively low data rates.

2. MODEL

We have developed an equilibrium model for (locally planar) boundary layers of the tangential discontinuity (TD) type. Strictly speaking, a tangential discontinuity—in which the magnetic field remains parallel to the current sheet surface throughout the interface layer—is an idealization as the normal magnetic field component always exhibits some stochastic and/or systematic deviations from zero. When these deviations are small enough (e.g., when microturbulence is present, or when the transition is a rotational discontinuity with a small normal component), however, the TD approximation is a useful one.

In order to model TD structure one must be able to represent the plasmas on either side of the current sheet ("outer populations") as well as those confined to the sheet ("inner populations"). This requires knowlege of the velocity distribution functions (VDFs). The model uses an analytical description of the VDFs that depends on a transition length parameter, which reflects the "sharpness" of the boundary. The model essentially consists of formulating the Vlasov-Maxwell equations, where the particle number densities and the current densities are obtained by analytically integrating the VDFs. The Vlasov-Maxwell equations are numerically solved by an adaptive-step numerical integrator. A detailed review of the model and some of its applications is given by Roth et al. (1996).

3. VALIDATION

The model involves a large number of physical quantities that are related to each other. For instance, given all the population densities, temperatures, bulk velocities and transition lengths, and given the magnetic field on one side of the transition, the model determines the number density, the magnetic field, the bulk velocity, and the electric field profiles throughout the current sheet. Alternatively, given these profiles, one may infer some properties of the particle populations, e.g., the inner populations about which not much is known in general (Whipple et al. 1984).

The validation of such a model consists of comparing observations with the current sheet structure computed with the model for a certain set of parameters. One can imagine two different situations: (a) there

Proc. 31st ESLAB Symp., 'Correlated Phenomena at the Sun, in the Heliosphere and in Geospace', ESTEC, Noordwijk, The Netherlands, 22-25 September 1997 (ESA SP-415, December 1997)

are not enough or barely sufficient observations to constrain all the model parameters, or (b) there are observational data in excess of those needed to fix the parameters. In the former case a weak form of validation of the model consists of checking whether it is possible to reproduce the observed internal current sheet structure by choosing reasonable values for the remaining free parameters; we will call this a test of the "realism" of the model. The latter case offers a direct way of verifying the relationships between various physical quantities incorporated in the model; it thus constitutes a "strong validation" of the model. In practice, the distinction between both cases is not very sharp as the number of model parameters is not uniquely defined. Indeed, the number of parameters is usually reduced a priori by making some additional physical assumptions. For instance, the model is often restricted to proton–electron plasmas. This limits the number of free parameters. Implicit is the assumption that, e.g., alpha particles play only a minor role. The validity of this assumption will usually not be addressed in the course of the validation process.

An additional validation technique consists of examining relationships between only a few parameters in the model. This can be done by fixing the values of some of the other parameters, and by eliminating parameters that do not strongly affect the particular relationship. A statistical survey of many transitions can then be used to test this derived relationship. We will call this process "indirect validation".

The validation of the current sheet model is hampered by the absence in many cases of plasma data with sufficiently high spatial resolution: transmission of full three-dimensional VDF measurements with sufficient resolution requires a high data rate. Some experiments (e.g., the plasma instrument aboard AMPTE/IRM (Paschmann et al. 1986)) circumvent this problem by performing on-board VDF moment calculations and transmitting only the moments at a high rate. In any case, knowledge of the form of the VDFs remains incomplete. High resolution magnetic field data, on the contrary, are routinely available.

3.1. Realism

A first type of validation is to see whether the model can explain the observed structure of the transition. That is: one tries to define particle populations (compatible with the limited plasma data) such that the model reproduces the observed high resolution magnetic field profile. Of course, one can always ameliorate the fit by adding populations. When the model is able to fit the observed profile with a minimal number of populations, we consider it to be "realistic".

An example of such a test is shown in Figure 1 (taken from (De Keyser et al. 1996)). We have used the model to reproduce the overall multi-layer structure of a broad solar wind discontinuity observed by ULYSSES at 4.57 AU and $-33.8°$ heliographic latitude in the high-speed solar wind. The magnetic field data rate is 1 vector per second; an ion 3-D spectrum is made once every 4 to 8 minutes. The plasma data can therefore be used only to characterize the outer populations (including in this case thermal electrons, protons, and alpha particles). Assuming the inner populations to have the same temperatures as the

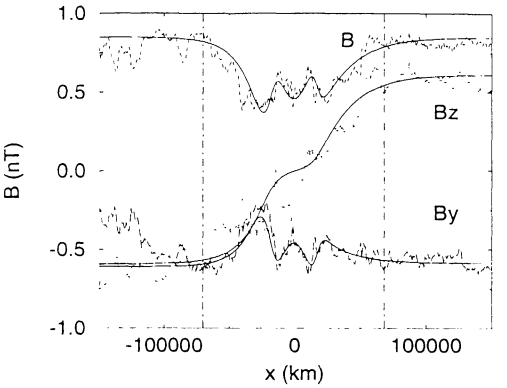

Figure 1. ULYSSES observations (dashed lines) and simulation (solid lines) of the magnetic field in the minimum variance frame (rotated over $-15°$ around the TD normal). The vertical lines delimit the TD crossing, centered at July 3, 5:29 UT, and lasting about 3 minutes. The horizontal axis gives the corresponding length scale along the TD normal. (Figure taken from De Keyser et al. 1996.)

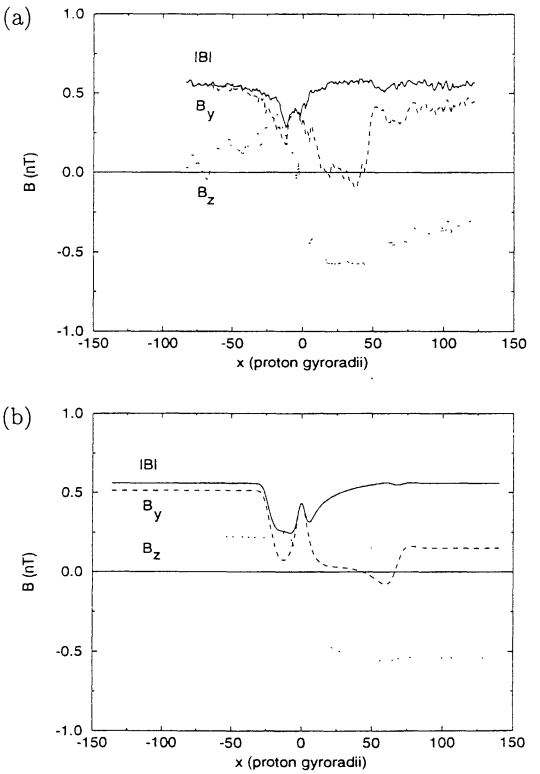

Figure 2. Comparison of (a) observed and (b) simulated magnetic field profiles for a polar solar wind TD encountered by ULYSSES on 1993, July 3, $11^h 40^m 00^s$. The plasmas on either side of the TD are the same; the current sheet is due to the presence of a velocity shear. (Figure taken from De Keyser et al. 1997.)

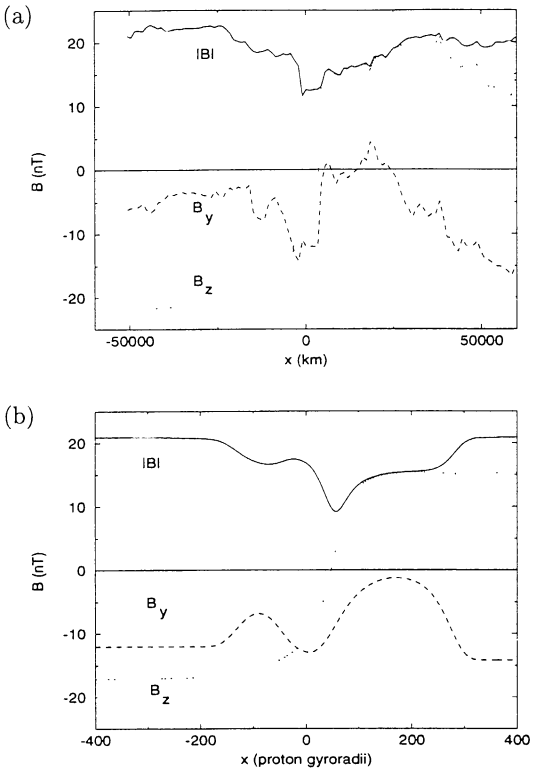

Figure 3. Comparison of (a) observed and (b) simulated magnetic field profiles for a WIND heliospheric current sheet crossing on 1994, December 6, $06^h 10^m 10^s$.

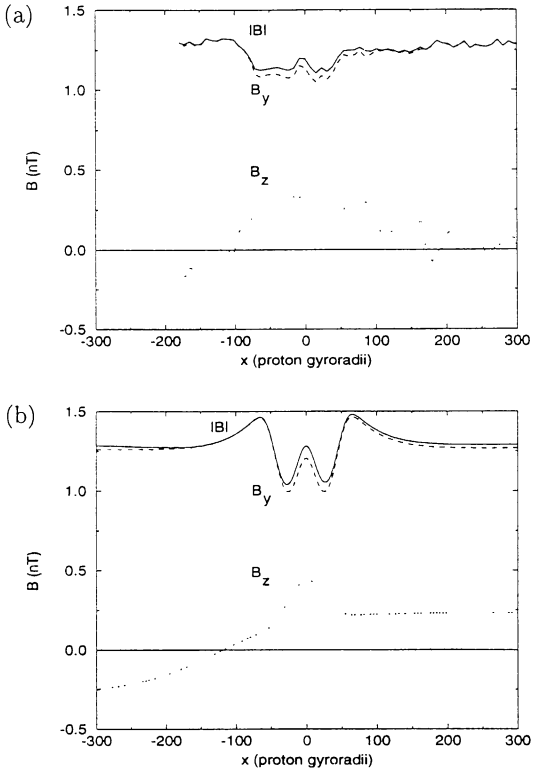

Figure 4. Comparison of (a) observed and (b) simulated magnetic field profiles for a polar solar wind nonlinear magnetic hole detected by ULYSSES on 1994, August 26, $01^h 40^m 10^s$, associated with the presence of a velocity shear between adjacent solar wind streams. (Figure taken from De Keyser et al. 1997.)

outer ones, pressure balance fixes the inner particle densities. Further choosing the transition lengths so as to match the observed length scales the magnetic field profile was successfully reproduced. The fine wavy-like structure superimposed on the overall profile is ascribed to turbulence. Propagation of waves across the TD can also be present.

Current sheet fine structure is particularly evident in transitions across which strong density, temperature, or velocity gradients exist. The effects of velocity shear are especially evident in the polar solar wind. ULYSSES observations have shown the solar wind to be rather uniform there (see, e.g., Feldman et al. 1996). In the absence of changes in composition, or strong density and temperature gradients, velocity shear effects are pronounced. De Keyser et al. (1997) have considered ULYSSES observations of several polar solar wind TDs. Figure 2 shows an example. It turns out that—given the plasma densities and temperatures and the magnetic field conditions on either side of the TD—the structure of the transition strongly depends on the velocity shear; the ion and electron transition lengths are two parameters influencing this relationship. For the observed velocity shear vectors (allowing for an uncertainty margin due to the low plasma data time resolution) one can always find appropriate values for the transition lengths for which much of the fine structure visible in the magnetic field profile is reproduced by the simulation.

A similar study was made using WIND observations of a heliospheric current sheet (HCS) crossing (Figure 3). In this particular case the plasmas on either side appeared to have the same characteristics; in general, however, strong density and temperature gradients are expected to exist across the HCS.

Another indication of the realism of the model is its ability to explain the existence and morphology of a particular kind of solar wind magnetic holes. Figure 4 (taken from (De Keyser et al. 1997)) compares ULYSSES observations and a simulation of a magnetic hole-like structure in the polar solar wind, i.e., a structure characterized by a significant magnetic field intensity depression across which almost no net magnetic field rotation is present. For the particular case of Figure 4, the model shows that the velocity shear across the interface is sufficient to create the observed density and magnetic field intensity variations across the transition.

Yet another illustration of the realism of the model is the fact that it can explain electron density enhancements observed in high magnetic shear crossings of the subsolar magnetopause (Hubert et al. 1997). Figure 5 demonstrates the good agreement between the magnetic field and the electron density profiles observed across the magnetopause by ISEE-1 and -2 (superposed epoch analysis of a 3-fold crossing, panels a–d) and those obtained from a model computation (panels e–h).

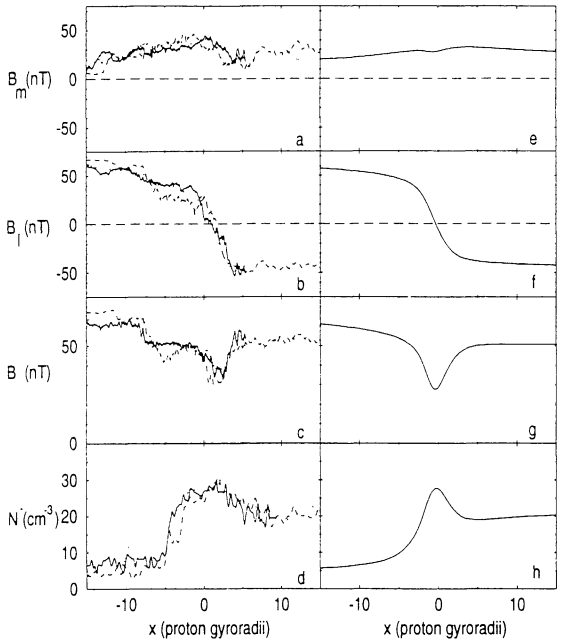

Figure 5. ISEE-1 observation and simulation of a 3-fold subsolar magnetopause crossing observed on August 30, 1981. The left panels (a)-(d) show the observed tangential magnetic field components B_m and B_l, the magnetic field intensity B, and the average electron density N^- between ISEE-1 and -2, in a superposed epoch plot. The right panels (e)-(h) show the results of a model computation. One should bear in mind that (d) represents the average electron density between both spacecraft, while (h) is the local density obtained from the model. Averaging necessarily leads to a broadening of the density peak. (Figure taken from Hubert et al. 1997.)

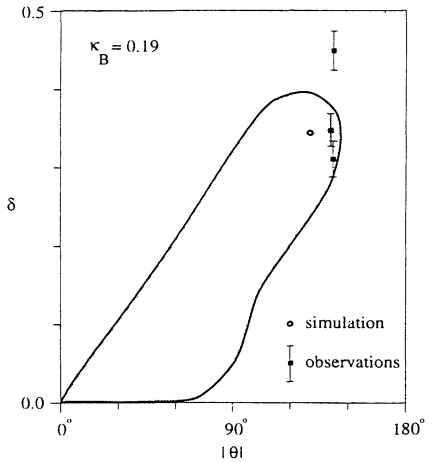

Figure 6. Theoretical variation of the density overshoot δ as a function of the magnetic field rotation angle θ for the subsolar magnetopause (magnetic field asymmetry $\kappa_B = 0.19$). The shaded area corresponds to equilibria obtained by varying the inner population parameters. In general, the density overshoot increases with the magnetic field rotation angle. The data points refer to the observations of the 3-fold crossing and the simulation presented in Figure 5. (Figure taken from Hubert et al. 1997.)

3.2. Strong Validation

Validation becomes a very strong test when independent observations are available for more physical quantities than there are parameters in the model.

An example of such a strong validation is the subsolar magnetopause analysis discussed above (Hubert et al. 1997). In this case, a radio sounding experiment between ISEE-1 and -2 (which were separated by a distance of only 220 km in the magnetopause normal direction, i.e., significantly less than the magnetopause thickness) permitted the determination of the integrated electron density along the trajectory between the satellites at a rate of 8 to 32 Hz. Both the magnetic field depression and the magnetic field rotation angle fix the kinetic pressure of the inner populations. The internal structure of the transition can then be computed without using the electron density data. The excellent agreement between the electron density profile predicted by the simulation and the one actually observed, as shown in Figure 5, therefore constitutes a very strong test of the model.

3.3. Indirect Validation

The current sheet model can be used to derive approximate relationships between some of its parameters, by fixing the other parameters or by letting them vary over a relevant range. The validity of the model can then be statistically tested by comparing these derived relationships with satellite observations of an important number of current sheets. We will illustrate this indirect validation by two examples.

Relation between magnetic shear and density fine-structure

Our model predicts a relationship between the kinetic pressure of the inner particles and the magnetic field rotation angle across the transition. Figure 6 shows this relationship for typical subsolar magnetopause crossings (Hubert et al. 1997). It is obtained by setting the plasma bulk velocities to zero on either side of the TD, by fixing the magnetic field asymmetry $\kappa_B = 1 - B^{msh}/B^{msph}$ (where B^{msh} and B^{msph} denote the magnetosheath resp. magnetospheric magnetic field strength), by taking the temperatures of the inner populations equal to those of the outer ones, and by varying other parameters (like, for instance, the orientation of the inner particle drift velocity, the values of the transition lengths) over a physically reasonable range. The shaded region in the figure shows the characteristics of the equilibria found from model computations for a given magnetic shear: the density overshoot $\delta = N^{peak}/N^{msh} - 1$ (where N^{peak} is the maximum density in the transition, and N^{msh} the magnetosheath density) can vary over a certain range. The figure marks the points corresponding to the three superposed crossings and the simulation of Figure 5; the points indeed do match the derived relationship. Unfortunately, the available sample of crossings was too small to test the relationship more thoroughly.

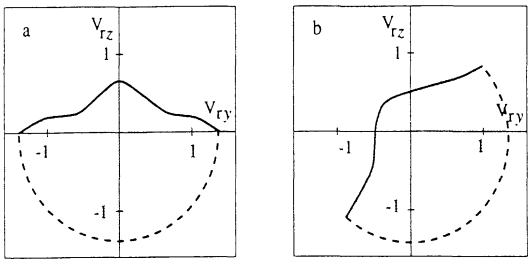

Figure 7. Velocity jump vector domains for which a TD equilibrium exists, for (a) symmetric and (b) asymmetric transitions. The domains sketch, for a fixed magnetic field rotation angle of +90°, the superposition of the domains obtained for a range of typical magnetosphere/magnetosheath plasma parameters. The dashed half-circle corresponds to the maximum velocity jump at the dayside magnetopause (derived from AMPTE/IRM observations). The velocity jump (V_{ry}, V_{rz}) is normalized to the magnetosheath ion thermal velocity. (Figure taken from De Keyser & Roth 1997c.)

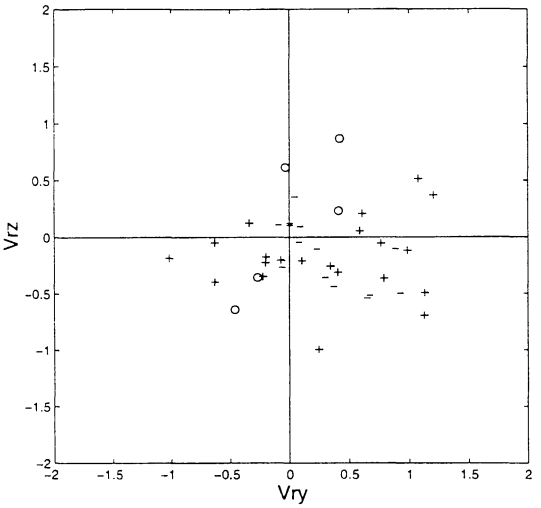

Figure 8. Plot of the velocity jump vector (V_{ry}, V_{rz}) (normalized to the magnetosheath ion thermal velocity) for a number of AMPTE/IRM magnetopause crossings. Low magnetic shear crossings ($|\theta| < 60°$) are indicated by a ∘ symbol, large positive magnetic field rotations ($\theta > 60°$) by a +, and large negative rotations ($\theta < -60°$) by a − symbol. (Figure taken from De Keyser & Roth 1997c.)

Relation between velocity shear and magnetic field configuration

We have used our model to determine, for prespecified plasma parameters and for a given magnetic field configuration, the set of bulk velocity shear vectors for which the current sheet may be in a state of TD equilibrium. It turns out that the model admits an equilibrium configuration only for a particular set of velocity shear vectors (De Keyser & Roth 1997a; De Keyser & Roth 1997b).

Figure 7 sketches the domain of velocity shear vectors for which an equilibrium exists. The TD surface coincides with the yz-plane; the y-axis has the direction of the inner bisectrix of the magnetic field vectors. The velocity shear (V_{ry}, V_{rz}) is normalized to the magnetosheath ion thermal velocity. Panel (a) has been obtained as the superposition of the domains obtained for various relevant choices of the plasma parameters (transition lengths, plasma densities and temperatures) and for a fixed magnetic field rotation angle (+90°), in the case of a symmetric transition (identical plasmas on either side of the TD); the shape of the domain, however, does not strongly depend on the precise value of the magnetic field rotation angle. Panel (b) considers asymmetric transitions; in this case, the domain is skewed to a certain degree, depending on the sense and the magnitude of the magnetic shear (again, the figure is made for a rotation of +90°). In either case the velocity shear domain covers only a limited fraction of the upper quadrants.

The velocity jump diagram of Figure 8 displays the observed velocity jump across the magnetopause as derived from AMPTE/IRM data (De Keyser & Roth 1997c). This figure presents a mix of magnetopause transitions in all sorts of regimes (different plasma properties) and with different magnetic field rotation angles. Points corresponding to large positive magnetic field rotations have been marked by + symbols, those with large negative rotations by − symbols, and low shear crossings (less than 60° magnetic field rotation) by ∘ symbols. It should be noted that the few low magnetic shear crossings in the upper quadrants are probably not in a state of TD equilibrium (for more details, see De Keyser & Roth 1997c), and therefore should be excluded when comparing observations with the TD theory. The observations (Figure 8) agree with the model (Figure 7) in the sense that the upper quadrants of the diagram are underpopulated indeed.

The above result can be reformulated (see Figure 9) in terms of regions on the magnetopause surface (hatched in the figure) where a given magnetic field rotation sense and magnitude can be observed (De Keyser & Roth 1997b; De Keyser & Roth 1997c). Figure 10 shows a GSM plot of the observed magnetic field rotation on a number of AMPTE/IRM passes. Crossings are indicated by a + (positive rotation) or a − symbol (negative rotation) with a size proportional to the magnitude of the rotation. There are several factors that complicate a direct comparison of this plot with Figure 9: Figure 9 was constructed for zero dipole tilt angle, deviations of the mean solar wind inflow direction may shift the location of the stagnation point, variations in magnetosheath and magnetospheric conditions lead to a varying degree of asymmetry of the transitions and alter the shape of the velocity shear domain. As a consequence, the demarcation lines of the regions where TD equilibrium may exist, are rather fuzzy. Nevertheless, the most important features of Figure 10 are in agreement with the model: the dominant presence of large positive magnetic field rotations north of the dawnside equator (dawnward of 9^h MLT), and the presence of low and high magnetic shear crossings with both positive and negative rotation sense near the stagnation point and toward the duskside. Also, low magnetic shear configurations do not occur dawnward of 9^h MLT (except for one non-TD low shear crossing). This agreement provides an indirect validation of the model. Observations at moderately high northern

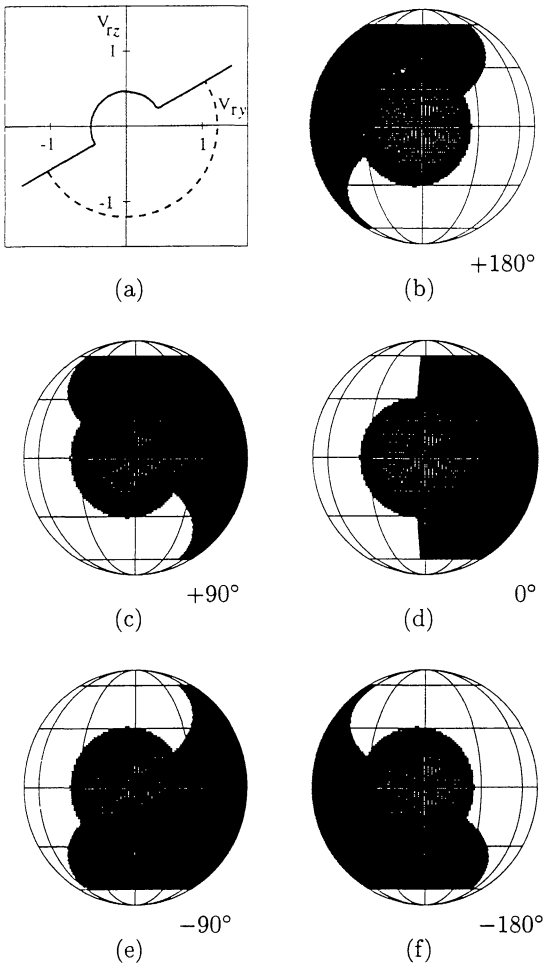

Figure 9. Given a typical velocity jump domain for asymmetric transitions as in panel (a) (see Figure 7b) and assuming that the magnetosheath plasma is streaming radially away from the stagnation point, it is possible to predict where the dayside magnetopause may be in TD equilibrium for a given magnetic field rotation angle. The stagnation point is at its typical location 5° dawnward from the subsolar point, and the dipole tilt angle is zero. The shaded regions correspond to magnetic field rotation angles of (b) +180°, (c) +90°, (d) 0°, (e) −90°, (f) −180°. (Figure taken from De Keyser & Roth 1997c).

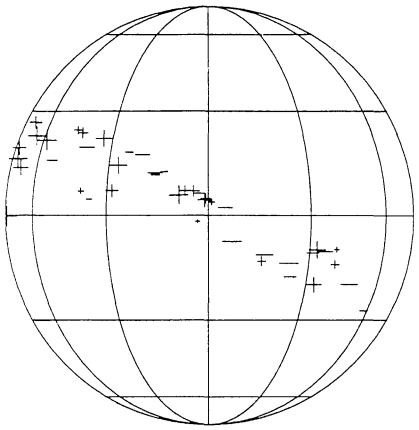

Figure 10. GSM map of AMPTE/IRM magnetopause crossings with the observed magnetic field rotation. A + symbol indicates a positive (clockwise) rotation, a − symbol a negative (counter-clockwise) rotation sense; the symbol size is proportional to the rotation angle. Note the dominant presence of large positive rotations north of the dawnside equator and the absence of low shear dawnside crossings (except for a case of questionable TD nature). Near the stagnation point and at the duskside both rotation senses are observed. (Figure taken from De Keyser & Roth 1997c).

and southern GSM latitudes near the noon meridian could further substantiate the model.

4. CONCLUSIONS

The validation of a current sheet model, which describes the relationships between a large number of physical quantities, is not a straightforward task. An important handicap is the lack of detailed information on the particle distributions. Observational tests involving solar wind current sheets (using ULYSSES and WIND data) and the magnetopause (using ISEE-1 and -2 and AMPTE/IRM data) cover a large enough sample of plasma conditions so as to ensure the validity of the current sheet model for a variety of regimes. Of course, during the validation one should keep the intrinsic limitations of the one-dimensional, time-independent Vlasov approach in mind. In particular, a Vlasov model of plane TDs does not have a unique solution, and it does not address the problem of particle accessibility (Whipple et al. 1984).

A validated model can be used for its predictive power: it can help to determine quantities that are hard to observe directly (e.g., space charge density, the electric field, inner population properties). By inferring, for instance, properties of the inner populations, one can derive constraints on the source and transport mechanisms of the populations. A validated equilibrium model is also the preferred starting point for establishing results on current sheet stability, since stability properties may depend critically on current sheet internal structure (Kuznetsova et al. 1994; Kuznetsova & Roth 1995).

ACKNOWLEDGMENTS

The authors thank B.T. Tsurutani and C.M. Ho (Jet Propulsion Lab, Caltech, Pasadena, CA, USA), A. Balogh (Imperial College, London, England), C.M. Hammond, J.L. Phillips, and D. McComas (Los Alamos National Laboratory, NM, USA) for ULYSSES data, A. Szabo, R. Lepping, and K. Ogilvie (Goddard Space Flight Center, Greenbelt, MD, USA) for WIND data, D. Hubert, C.C. Harvey (Département de Recherche Spatiale, Observatoire de Paris-Meudon, France) and C.T. Russell (Institute of Geophysics and Planetary Physics, University of California, Los Angeles, CA, USA) for ISEE-1 and -2 data, D. Sibeck (Johns Hopkins University, Laurel, MD, USA), G. Paschmann (Max-Planck-Institut für Extraterrestrische Physik, Garching, Germany), H. Lühr (Institüt für Geophysik und Meteorologie, Technische Universität Braunschweig, Germany) for AMPTE/IRM data. The authors are also indebted to J.F. Lemaire and M.M. Kuznetsova for fruitful discussions. Part of this work was supported by the ESA (PRODEX) project "Interdisciplinary Study of Directional Discontinuities" as part of the ULYSSES mission. We acknowledge the support of the Belgian Federal Services for Scientific, Technical and Cultural Affairs.

REFERENCES

De Keyser, J., Roth, M., Lemaire, J. et al., 1996, Theoretical plasma distributions consistent with ULYSSES magnetic field observations in a high-speed solar wind tangential discontinuity, Solar Phys., 166, 415

De Keyser, J., Roth, M., Tsurutani, B.T. et al., 1997, Solar wind velocity jumps across tangential discontinuities: ULYSSES observations and kinetic interpretation, A&A, 321, 945

De Keyser, J., Roth, M., 1997, Equilibrium conditions for the tangential discontinuity magnetopause, J. Geophys. Res., 102, 9513

De Keyser, J., Roth, M., 1997, Equilibrium conditions and magnetic field rotation at the tangential discontinuity magnetopause, J. Geophys. Res., submitted

De Keyser, J., Roth, M., 1997, Magnetic field rotation at the dayside magnetopause: AMPTE/IRM observations, J. Geophys. Res., submitted

Feldman, W.C., Barraclough, B.L., Phillips, J.L. et al., 1996, Constraints on high-speed solar wind structure near its coronal base: a ULYSSES perspective, A&A, 316, 355

Hubert, D., Harvey, C.C., Roth, M. et al., 1997, Electron density at the subsolar magnetopause for high magnetic shear: ISEE 1 and 2 observations, J. Geophys. Res., submitted

Kuznetsova, M.M., Roth, M., Wang, Z. et al., 1994, Effect of the relative flow velocity on the structure and stability of the magnetopause current layer, J. Geophys. Res., 99, 4095

Kuznetsova, M.M., Roth, M., 1995, Thresholds for magnetic percolation through the magnetopause current layer in asymmetrical magnetic fields, J. Geophys. Res., 100, 155

Paschmann, G., Papamastorakis, I., Baumjohann, W. et al., 1986, The magnetopause for large magnetic shear: AMPTE/IRM observations, J. Geophys. Res., 91, 11099

Roth, M., De Keyser, J., Kuznetsova, M.M., 1996, Vlasov theory of the equilibrium structure of tangential discontinuities in space plasmas, Space Sci. Rev., 76, 251

Whipple, E.C., Hill, J.R., Nichols, J.D., 1984, Magnetopause structure and the question of accessibility, J. Geophys. Res., 89, 1508